

## Inelastic Cross Section for $p$ -Air Collisions from Air Shower Experiments and Total Cross Section for $p$ - $p$ Collisions up to $\sqrt{s} = 24$ TeV

M. Honda,<sup>(1)</sup> M. Nagano,<sup>(1)</sup> S. Tonwar,<sup>(2)</sup> K. Kasahara,<sup>(3)</sup> T. Hara,<sup>(4)</sup> N. Hayashida,<sup>(1)</sup>  
Y. Matsubara,<sup>(5)</sup> M. Teshima,<sup>(1)</sup> and S. Yoshida<sup>(6)</sup>

<sup>(1)</sup>*Institute for Cosmic Ray Research, University of Tokyo, Tanashi, Tokyo, Japan*

<sup>(2)</sup>*Tata Institute of Fundamental Research, Homi Bhabha Marg, Colaba, Bombay, India*

<sup>(3)</sup>*Faculty of Engineering, Kanagawa University, Kanagawa, Japan*

<sup>(4)</sup>*Yuge National College of Maritime Technology, Yuge, Ehime, Japan*

<sup>(5)</sup>*Cosmic Ray Section, STE Laboratory, Nagoya University, Nagoya 464, Japan*

<sup>(6)</sup>*Department of Physics, Tokyo Institute of Technology, Ohokayama, Tokyo, Japan*

(Received 25 September 1992)

Based on an analysis of the extensive air shower data accumulated over the last ten years at Akeno Cosmic Ray Observatory, the value of the proton-air nuclei inelastic cross section ( $\sigma_{in}^{p-air}$ ) has been determined assuming the validity of quasi-Feynman scaling of particle production in the fragmentation region. The energy dependence of  $\sigma_{in}^{p-air}$  can be represented as  $290(E/1 \text{ TeV})^{0.052}$  mb in the energy interval  $10^{16.2}-10^{17.6}$  eV, where  $E$  is the incident proton energy. The total  $p$ - $p$  cross section ( $\sigma_{tot}^{p-p}$ ), derived using the nuclear distribution function obtained from the shell model, increases with energy as  $38.5 + 1.37 \ln^2(\sqrt{s}/10 \text{ GeV})$  mb.

PACS numbers: 13.85.Tp, 13.85.Lg, 25.40.Ve, 96.40.Pq

Cosmic ray experiments provide us with a unique opportunity to measure the inelastic cross section ( $\sigma_{in}^{p-air}$ ) for proton-air-nucleus interactions at ultrahigh energies ( $E \sim 10^{17}$  eV). At present, accelerator data are available only up to  $\sqrt{s} = 1.8$  TeV for  $\bar{p}$ - $p$  interactions. In our earlier papers [1,2] based on data from the extensive air shower (EAS) experiment at Akeno, 150 km west of Tokyo (hereafter referred to as I and II, respectively), we have reported the energy dependence of  $\sigma_{in}^{p-air}$  as  $290(E/1 \text{ TeV})^{0.066}$  mb for the incident proton energy ( $E$ ) interval  $10^{15.3}-10^{17.4}$  eV. The energy dependence of the total  $p$ - $p$  cross section ( $\sigma_{tot}^{p-p}$ ) was also presented in II as  $38.5 + 1.84 \ln^2(\sqrt{s}/10 \text{ GeV})$  mb. This was derived assuming the validity of geometrical scaling and Glauber theory at these ultrahigh energies.

The procedure for measuring the inelastic cross section ( $\sigma_{in}^{p-air}$ ) from air shower data is as follows. The frequency dependence of EASs on zenith angle is determined for air showers with a given total number of electrons ( $N_e$ ) and muons ( $N_\mu$ ). It is assumed that all air showers with a given  $N_e$  and  $N_\mu$  have developed through the same column density along the path and have been initiated by primary particles of the same primary energy  $E_0$ . Under these assumptions, the observed mean free path  $\lambda_{obs}$  can be determined from

$$f(N_e, N_\mu, \theta) = f(N_e, N_\mu, 0) \exp\{-x_0(\sec\theta - 1)/\lambda_{obs}\}, \quad (1)$$

where  $f(N_e, N_\mu, \theta)$  is the rate of showers of a given  $N_e$  and  $N_\mu$  at zenith angle  $\theta$  and  $x_0$  is the atmospheric depth for the observation level (920 g/cm<sup>2</sup> at Akeno).

The mean free path  $\lambda_{obs}$ , thus determined, would be different for different nuclear species in the primary cosmic ray flux. To determine  $\lambda_{obs}$  for protons, we used a selection procedure for showers in I to enrich the data sample with proton initiated showers. Any contamination

of the data sample by showers initiated by heavier nuclei tends to make  $\lambda_{obs}$  smaller. However, simulations have shown that if there are more than 15% protons in primary flux and the number of helium nuclei is less than 10%, the contribution of heavier nuclei is insignificant for determination of the value of  $\lambda_{obs}$ .

On the other hand, the fluctuations in the longitudinal development of air showers make  $\lambda_{obs}$  larger than the true collision mean free path  $\lambda_{in}$ . Parametrizing the relation as  $\lambda_{obs} = k\lambda_{in}$ , the value of  $k$  was estimated through Monte Carlo simulations. The value of  $k$ , used in I and II, was obtained with the assumption that there is no significant break of Feynman scaling in the fragmentation region ( $x \geq 0.05$ ) and that the multiplicity increases as  $\ln^2 s$ . If we assume a breakdown of scaling in the fragmentation region, a smaller value of  $k$  is expected.

At the Akeno observatory, the extensive air shower experiment started at the end of 1979 with much improved accuracies in determination of both  $N_e$  and  $N_\mu$  for individual showers compared to earlier experiments. The experiment has continued without any change in the triggering criteria for showers of energy above  $10^{16}$  eV during the last ten years. We have now accumulated 4 times more showers compared to data used for results presented in I and II. In the present analysis, we are able to use 2 times larger effective collection area for showers, which is made possible by limiting the lowest energy to  $10^{16}$  eV. With an 8 times larger data set compared to I, we are now able to select showers whose maxima of development are closer to the observational level and reduce possible systematic errors.

The details of the Akeno EAS array have been described elsewhere [3] and we discuss here only the salient features of the array relevant to the present analysis. The array consists of 156 detectors, each 1 m<sup>2</sup> in area. These

detectors are distributed over 1 km<sup>2</sup> area with detector spacing of 120 m. There are three clusters of detectors in the array with (90×90) m<sup>2</sup> area each which have closely spaced (30 m) detectors to facilitate observation of showers of size less than 10<sup>6.5</sup>. Nine muon detectors, each 25 m<sup>2</sup> in area and spread over the area of the EAS array, have been used for determination of  $N_\mu$  in a shower. The threshold energy for the muon detectors is  $(1 \times \sec\theta)$  GeV, where  $\theta$  is the zenith angle of the muon.

The trigger for showers used in the present analysis required a signal from any 7 or more of the 38 triggering detectors having 120 m separation between them, giving a rate of about 20 per hour. The total effective observation time used for the present analysis is  $2.2476 \times 10^8$  s ( $\sim 7.16$  yr), which is nearly 4 times compared to I. Of the  $1.4 \times 10^6$  showers recorded during this period, the cores of 625 567 showers were incident within the array. 553 065 showers with cores incident inside a fiducial area of (700×600) m<sup>2</sup> and zenith angle less than 48.2° ( $\sec\theta \leq 1.5$ ) have been used for the analysis discussed below.

To determine  $N_e$  for individual showers, the Nishimura-Kamata-Greisen (NKG) function [4] has been used for the lateral distribution of shower particles, with a variable age parameter. For showers of sizes around 10<sup>7</sup>, particle densities from more than 70 detectors are available for the fit to the NKG function and this number increases to more than 120 for showers of size  $\sim 10^8$ .

$N_\mu$  is calculated by fitting the observed muon densities to the function given by Greisen [5] with a characteristic length of  $r_0 = (280 \pm 20)$  m [6]. Detectors within 50 m from the core are excluded from the fit in order to avoid the contamination from the punch throughs of the energetic electron-photon component.

The error ( $\sigma$ ) in the determination of zenith angle in the large- $N_e$  region considered here has been estimated to be 3.0°. The errors in determination of  $\log_{10} N_e$  and  $\log_{10} N_\mu$  are 0.05 and 0.1, respectively.

Since the attenuation of  $N_\mu$  is very slow after its maximum development,  $N_\mu$  is considered to be a good estimator of primary energy  $E_0$ .  $E_0$  is represented by  $N_\mu$  as [7]

$$E_0 \text{ (eV)} = 1.17 \times 10^{17} (N_\mu / 10^6)^{1.2}. \tag{2}$$

For the same primary energy, the observed  $N_\mu$  attenu-

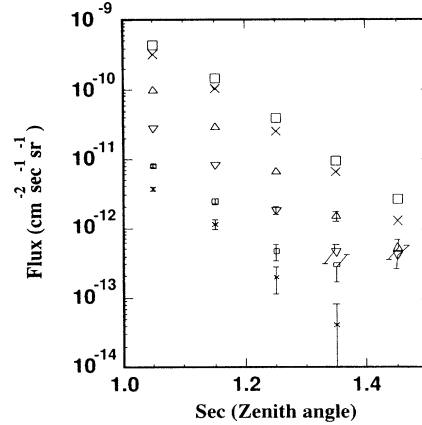


FIG. 1. Zenith angle dependence of the flux of showers which have the constant  $(N_\mu, N_e)$ . Boxes show the flux with  $[\log_{10}(N_\mu), \log_{10}(N_e)] = (5.25-5.45, 6.8-7.0)$ , crosses (5.45-5.65, 7.0-7.3), upper triangles (5.65-5.86, 7.3-7.6), lower triangles (5.85-6.05, 7.6-7.9), small boxes (6.05-6.25, 7.9-8.2), and small crosses (6.25-6.45,  $\geq 8.1$ ).

ates with zenith angle. This is due to the change in the threshold energy of detected muons as  $(1 \times \sec\theta)$  GeV and the increase of decay probability of muons with zenith angle. Therefore we use the zenith angle dependent  $N_\mu(\theta)$  to select showers of constant energy. This can be made by evaluating the size at constant intensity of integral  $N_\mu(\theta)$  spectrum for each zenith angle bin. If we express attenuation length ( $\Lambda_\mu$ ) of  $N_\mu$  by

$$N_\mu(\theta) = N_\mu(0) \exp[-920(\sec\theta - 1)/\Lambda_\mu], \tag{3}$$

$\Lambda_\mu$  obtained between  $\sec\theta = 1.0$  and 1.5 is  $(1100 \pm 100)$  g/cm<sup>2</sup>.

In Fig. 1, the zenith angle distribution of showers with constant  $(N_\mu, N_e)$  are plotted for six  $N_\mu$  ranges.  $N_e$  bin is chosen to be about (5-10)% of showers from the largest  $N_e$  for a fixed  $N_\mu$  bin. This permits a preferential selection of showers which are close to their maximum development near the Akeno level. The values for  $\lambda_{\text{obs}}$  have been calculated from a weighted least-squares fit of the zenith angle distribution of showers with constant  $(N_\mu, N_e)$  by Eq. (1). The results are listed in the fourth column of Table I.

TABLE I. The list of  $N_\mu$ ,  $N_e$ , primary energy,  $\lambda_{\text{obs}}$ ,  $\lambda_{\text{obs}}^{\text{air}}$ ,  $\sigma_{\text{obs}}$ , and  $\sigma_{\text{in}}^{\text{air}}$ . For the definitions and derivations, see the text.

$\log_{10} N_\mu$	$\log_{10} N_{10}$	$\log_{10} E_0$ (eV)	$\lambda_{\text{obs}}$ (g/cm <sup>2</sup> )	$\lambda_{\text{obs}}^{\text{air}}$ (g/cm <sup>2</sup> )	$\sigma_{\text{obs}}$ (mb)	$\sigma_{\text{in}}^{\text{air}}$ (mb)
5.25-5.45	6.8-7.0	16.17-16.41	78.2 ± 4.7	75.2 ± 4.7	320 ± 20	480 ± 33
5.45-5.65	7.0-7.3	16.41-16.65	75.9 ± 5.1	72.9 ± 5.1	333 ± 23	500 ± 38
5.65-5.85	7.3-7.6	16.65-16.89	70.3 ± 3.8	67.3 ± 3.8	358 ± 20	537 ± 33
5.85-6.05	7.6-7.9	16.89-17.13	74.3 ± 7.9	71.3 ± 7.9	338 ± 37	507 ± 61
6.05-6.25	7.9-8.2	17.13-17.37	75.5 ± 8.6	72.5 ± 8.6	332 ± 40	498 ± 64
6.25-6.45	$\geq 8.1$	17.37-17.61	68.7 ± 7.9	65.7 ± 7.9	367 ± 44	550 ± 72

The error in the zenith angle determination makes  $\lambda_{\text{obs}}$  larger than the real value. This difference has been evaluated assuming the dispersion  $\sigma(\theta)$  in the determination of zenith angle to be a Gaussian. For the present case, we have obtained the relation,  $\lambda_{\text{obs}}^c = \lambda_{\text{obs}} - 3$  ( $\text{g}/\text{cm}^2$ ) with  $\sigma(\theta) = 3.0^\circ$ , which is found to be independent of the value of  $\theta$  up to  $48.2^\circ$ .

The cross section  $\sigma_{\text{obs}}$  has been calculated using the relation

$$\sigma_{\text{obs}} (\text{mb}) = 2.41 \times 10^4 / [\lambda_{\text{obs}}^c (\text{g}/\text{cm}^2)]. \quad (4)$$

The values of  $\lambda_{\text{obs}}^c$  and  $\sigma_{\text{obs}}$  are listed in the fifth and sixth columns of Table I, respectively. The values of  $p$ -air cross section,  $\sigma_{\text{in}}^{p\text{-air}}$ , obtained from  $\sigma_{\text{obs}}$  using the correction factor  $k = 1.5$ , which was estimated in I, are listed in the seventh column of Table I. The errors shown in Table I are statistical only as obtained from the least-squares fit while determining  $\lambda_{\text{obs}}$ . The energy dependence of  $\sigma_{\text{in}}^{p\text{-air}}$  is expressed by

$$\sigma_{\text{in}}^{p\text{-air}} = 290(E/1 \text{ TeV})^{0.052} \text{ mb}, \quad (5)$$

in the energy interval  $10^{16.2} - 10^{17.6}$  eV.

The  $\sigma_{\text{in}}^{p\text{-air}}$  values shown in Table I are plotted in Fig. 2 for a comparison with the results obtained from other cosmic ray experiments. It is seen that the  $\sigma_{\text{in}}^{p\text{-air}}$  values obtained from the distribution of shower maxima [8] agree well with our values. The lower limits determined from the surviving proton flux [9] (YPT) and the Mt. Fuji emulsion experiment [10] (FUJI) are shown as line segments in Fig. 2.

In this analysis, the stage of shower development has been assumed to be the same for all showers with fixed  $(N_\mu, N_e)$  irrespective of the atmospheric depth. Since the lateral distribution of electrons reflects the stage of the longitudinal development of shower, the dependence of the average age on  $N_e$  has been examined for different

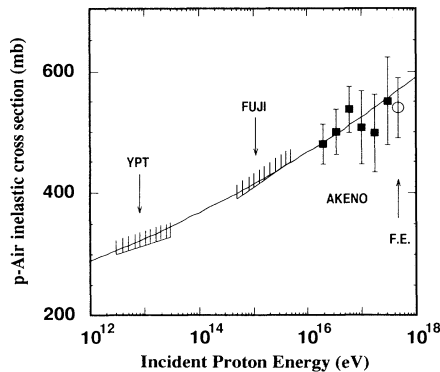


FIG. 2. Energy dependence of  $\sigma_{\text{in}}^{p\text{-air}}$  on incident proton energy. Present analysis (solid boxes); FE denote  $\sigma_{\text{in}}^{p\text{-air}}$  obtained by Fly's Eye group [8]; YPT [9] and FUJI [10] represent the lower limits on  $\sigma_{\text{in}}^{p\text{-air}}$  from the surviving proton flux at Mt. Chacaltaya and from the Mt. Fuji emulsion chamber experiment, respectively; the solid line represents best fit curve in the form of  $\sigma_{\text{in}}^{p\text{-air}} = 290(E/1 \text{ TeV})^\alpha \text{ mb}$  with  $\alpha = 0.052$ .

zenith angle bins for a fixed  $N_\mu$ . It has been found that the average age has only a weak dependence on the zenith angle for fixed  $N_e$  and  $N_\mu$ . The rate of change of shower age with depth is  $(-0.01 \pm 0.005/100) \text{ g cm}^{-2}$ , which is much smaller than the value  $(+0.04 \pm 0.006/100) \text{ g cm}^{-2}$  obtained for showers with fixed  $N_\mu$  without any selection on  $N_e$ . This suggests that showers of fixed  $N_e$  and  $N_\mu$  are in a similar stage of longitudinal development irrespective of zenith angles.

The proportion of showers produced by primary protons is unknown among showers selected using constant  $N_\mu$ . In order to optimize selection of showers which have a larger probability of being produced by primary proton, we have selected showers of  $N_e$  larger than a value  $N_e^{\text{th}}$  for a fixed  $N_\mu$ . If we define a parameter  $R$  as the fraction of showers with  $N_e$  larger than  $N_e^{\text{th}}$  to total number of showers with a fixed  $N_\mu$ , we find that the value of  $\lambda_{\text{obs}}$  remains constant, within experimental errors, for different values of  $R$  up to around  $R = 10\%$  and increases thereafter as  $R$  increases above  $10\%$ . This suggests that the proportion of protons does not change significantly at least up to  $R = 10\%$ . The existence of more than  $10\%$  protons in the primary beam in the  $3 \times 10^{17}$  eV region is supported by the depth distribution of the maximum shower development observed by the Fly's Eye detectors operating in stereo mode [11].

We have derived the values for  $\sigma_{\text{tot}}^{p\text{-}p}$  from inelastic cross-section values following Glauber theory [12] and assuming geometrical scaling [13] as discussed in II. This derivation is closely related to the assumption for the profile function for  $p$ - $p$  interactions and its energy dependence. For the present analysis, we have employed the profile function used by Durand and Pi [14] who have calculated the energy dependence of  $\sigma_{\text{tot}}^{p\text{-}p}$  based on QCD. They also have applied their calculations to  $\sigma_{\text{tot}}^{p\text{-air}}$  employing the shell model for the nucleon distribution in the nucleus.

In Fig. 3, we have shown the relationship between  $\sigma_{\text{tot}}^{p\text{-}p}$

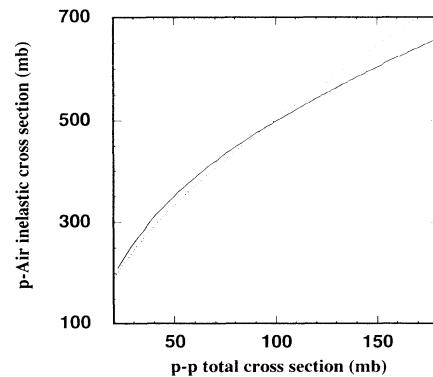


FIG. 3. The relation between  $\sigma_{\text{tot}}^{p\text{-}p}$  and  $\sigma_{\text{in}}^{p\text{-air}}$ . The solid curve shows the result obtained using the method given by Durand and Pi [14] and the dotted curve shows the relation with geometrical scaling and Glauber theory.

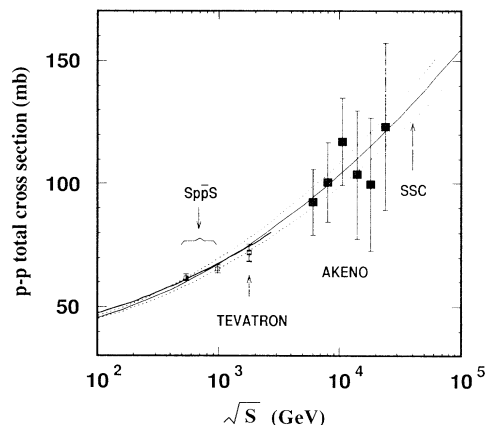


FIG. 4. Energy dependence of  $\sigma_{\text{tot}}^{p-p}$  obtained using the method given by Durand and Pi (large solid boxes) and its comparison with the results of  $\sigma_{\text{tot}}^{p-p}$  obtained from the accelerator data [15–17] (small boxes). The thin line shows the best fit curve in the form of  $\sigma_{\text{tot}}^{p-p} = 38.5 + \alpha \ln^2(\sqrt{s}/10 \text{ GeV})$  with  $\alpha = 1.37$ . The dotted lines correspond to 1 standard deviated values of  $\alpha$  from the best fit value. The thick line shows the extrapolation of the least-squares fit to the accelerator data up to Tevatron energies [18].

and  $\sigma_{\text{in}}^{p-\text{air}}$  following the calculations of Durand and Pi. For a comparison, we have also plotted in the same figure the curve obtained by assuming the validity of geometrical scaling. The profile function used by Durand and Pi increases its central density as the proton cross section increases, while in the case of geometrical scaling, the profile function expands in the radial direction while keeping the central density constant. It is interesting that although the profile functions are so different, the difference in cross-section values is not so large. Especially, in the range of  $\sigma_{\text{tot}}^{p-p} \sim 120 \text{ mb}$ , which is of interest here, the agreement between the two calculations is indeed very good.

In Fig. 4, we have plotted  $\sigma_{\text{tot}}^{p-p}$  values obtained by using the nucleon profile function given by Durand and Pi. The best fit curve shown in Fig. 4 represents the relation

$$\sigma_{\text{tot}}^{p-p} = 38.5 + \alpha \ln^2(\sqrt{s}/10 \text{ GeV}) \quad (6)$$

with a value of 1.37 for  $\alpha$ . Under the assumption of geometrical scaling, we get a very similar result with  $\alpha = 1.33$ . In the same figure, we have also plotted  $\sigma_{\text{tot}}^{\bar{p}-p}$  values given by the collider experiments [15–17] and the curve fitted up to Fermilab Tevatron energy given by the Particle Data Group [18]. The energy dependence of  $\sigma_{\text{tot}}^{p-p}$  is also fitted as  $\sigma_{\text{tot}}^{p-p} = 38.5 \times (E/1 \text{ TeV})^{0.091}$  for incident proton energy  $E$ .

It is seen from Fig. 4 that the value of  $\sigma_{\text{tot}}^{p-p}$  is expected to be  $133 \pm 10 \text{ mb}$ , not including the conversion uncertainty from  $\sigma_{\text{in}}^{p-\text{air}}$  to  $\sigma_{\text{tot}}^{p-p}$ , at the design energy ( $\sqrt{s} = 40 \text{ TeV}$ ) for the Superconducting Super Collider (SSC).

We have presented here our results on the inelastic cross section for  $p$ -air collisions up to energies of  $10^{17.6}$

eV as determined from data obtained from the Akeno air shower experiment. Using these values we have derived the values for the total cross section for  $p$ - $p$  collisions expected at SSC energy. Our best fit curve is a little higher than the extrapolation of  $\sigma_{\text{tot}}^{p-p}$  values from the CERN SppS and Tevatron colliders. We note that our results are somewhat dependent on the model for hadronic interactions assumed for calculating the correction factor  $k$ . The value of  $k$  is expected to become a little smaller and hence  $\sigma$  also become smaller if there is a significant breakdown of scaling in the fragmentation region.

We acknowledge with thanks the valuable contributions of other members of the Akeno Group in the construction and operation of the array. We are grateful to Professor J. Arafune for his kind suggestions. The analysis was carried out with the FACOM M780 at the Institute for Nuclear Study, University of Tokyo.

- [1] T. Hara *et al.*, Phys. Rev. Lett. **50**, 2058 (1983).
- [2] T. Hara *et al.*, in *Proceedings of the Eighteenth International Cosmic Ray Conference, Bangalore, 1983*, edited by N. Durgaprasad *et al.* (Indian National Scientific Documentation Center, New Delhi, India, 1983), Vol. 11, p. 354.
- [3] T. Hara *et al.*, in *Proceedings of the Sixteenth International Cosmic Ray Conference, Kyoto, 1979* (University of Tokyo, Tokyo, Japan, 1979), Vol. 8, p. 135.
- [4] K. Greisen, in *Progress in Cosmic Ray Physics III*, edited by J. G. Wilson (North-Holland, Amsterdam, 1956), p. 27.
- [5] K. Greisen, Phys. Rev. Lett. **16**, 748 (1966).
- [6] N. Jogo, Ph.D. thesis, University of Tokyo, 1981.
- [7] M. Nagano *et al.*, J. Phys. G **10**, 1295 (1984).
- [8] R. M. Baltrusaitis *et al.*, in *Proceedings of the Nineteenth International Cosmic Ray Conference, La Jolla, 1985*, edited by F. C. Jones (Goddard Space Flight Center, Greenbelt, MD, 1985), Vol. 6, p. 252.
- [9] G. B. Yodh *et al.*, Phys. Rev. Lett. **28**, 1005 (1972).
- [10] M. Akashi *et al.*, Phys. Rev. D **24**, 2353 (1981).
- [11] G. L. Cassiday *et al.*, Astrophys. J. **356**, 669 (1990).
- [12] R. J. Glauber, in *Lecture in Theoretical Physics*, edited by W. Britten and L. G. Dunham (Interscience, New York, 1959), Vol. 1, p. 315; R. J. Glauber and G. Matthiae, Nucl. Phys. **B21**, 135 (1970).
- [13] V. Barger, J. Luthe, and R. J. N. Phillips, Nucl. Phys. **B88**, 237 (1975), and references therein.
- [14] L. Durand and H. Pi, Phys. Rev. D **38**, 78 (1988).
- [15] UA4 Collaboration, M. Bozzo *et al.*, Phys. Lett. **B147**, 392 (1984); UA4 Collaboration, D. Bernard *et al.*, Phys. Lett. **B 198**, 583 (1987).
- [16] UA5 Collaboration, G. J. Alner *et al.*, CERN Report No. CERN-EP/86-57, 1986 (unpublished).
- [17] E710 Collaboration, N. A. Amos *et al.*, Phys. Lett. **B 243**, 158 (1990); CDF Collaboration, S. White *et al.*, in *The International Conference on Elastic and Diffractive Scattering*, Proceedings of the Fourteenth Blois Workshop, Elba, Italy, 1991, edited by F. Cavelli and S. Zucchelli [Nucl. Phys. B (Proc. Suppl.)].
- [18] Particle Data Group, K. Hikasa *et al.*, Phys. Rev. D **45**, III.83 (1992).